A Letters Journal Exploring the Frontiers of Physics

July 2015

EPL, **111** (2015) 27005
doi: 10.1209/0295-5075/111/27005

www.epljournal.org

Speed of field-driven domain walls in nanowires with large transverse magnetic anisotropy

M. C. Depassier

Instituto de Física, Pontificia Universidad Católica de Chile - Casilla 306, Santiago 22, Chile

received 7 May 2015; accepted in final form 20 July 2015
published online 17 August 2015

PACS 75.78.-n – Magnetization dynamics
PACS 75.78.Fg – Dynamics of domain structures
PACS 75.75.-c – Magnetic properties of nanostructures

Abstract – Recent analytical and numerical work on field-driven domain wall propagation in nanowires and thin films has shown that for large transverse anisotropy and sufficiently large applied fields the Walker profile becomes unstable before the breakdown field, giving way to a domain wall whose speed increases at a slower rate with the applied field. We perform an asymptotic expansion of the Landau-Lifshitz-Gilbert equation for large transverse magnetic anisotropy and show that the asymptotic dynamics reproduces this behavior. The appearance of a different regime in the asymptotic dynamics is due to a transition from a pushed to a pulled front of a reaction diffusion equation in which the speed of the domain wall increases with the square root of the applied field

Magnetic domain wall propagation is an active area of research both as an interesting physical phenomenon as well as for its possible applications in logic devices, magnetic memory elements and others [1]. The dynamics of magnetic domain walls is described by the Landau-Lifshitz-Gilbert (LLG) equation [2,3] which cannot be solved analytically except in very special cases. For an infinite medium with uniaxial anisotropy and an external field applied along the symmetry axis, the Walker solution [4] provides the best-known analytical expression for the profile and speed of the domain wall. The exact Walker solution, predicts that the speed increases linearly with the field up to a critical field H_w. Above this value a sudden drop in velocity and an irregular precessing motion of the magnetization appears. Field-induced domain wall propagation in thin films and nanowires has been examined with greater detail in recent work. The numerical study [5] showed that depending on the relative magnitude of the hard-axis anisotropy different scenarios arise. For small hard-axis anisotropy the Walker solution is realized. For sufficiently large values of the hard-axis anisotropy the Walker breakdown does not occur. There is a slower increase in speed of the domain wall due to spin wave emission and no sudden drop in speed. For the largest values considered in [5] the domain wall speed changes from a regime of linear growth with the applied field to a regime of slower growth with increasing applied field. This behavior is observed when both the exchange constant and uniaxial anisotropy are much smaller than the hard-axis anisotropy. Further numerical studies [6,7] analyze in detail the nature of the spin waves emitted and distinguish two scenarios, depending on the relative values of the exchange and anisotropy constants. The parameter ranges studied in [5] and [7] differ, however, in both cases the Walker breakdown is not observed when the hard-axis anisotropy is sufficiently large. The stability of the Walker solution with respect to small perturbations has been studied recently [8] using dynamical systems techniques. The analysis of the spectrum of a perturbation to the Walker solution shows that it may become absolutely or convectively unstable before the breakdown field. This instability is found for sufficiently large hard-axis anisotropy and for fields larger than a critical value. Samples with a large disparity in anisotropies have been achieved in the magnetic semiconductor (Ga, Mn)(As, P) [9] showing that the ratio of anisotropies has a large effect on the domain wall speed in agreement with the numerical calculations mentioned above.

The purpose of this work is to study the dynamics of the LLG equation by means of an asymptotic expansion using as a small parameter the ratio between easy- and hard-axis anisotropies. The asymptotic expansion captures the slower relaxation dynamics of the domain wall and filters out the fast spin waves [10]. We find that the leading-order

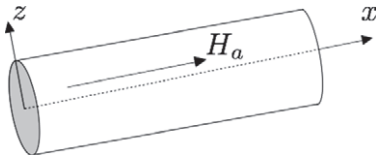

Fig. 1: Coordinate axes and applied field in the nanowire.

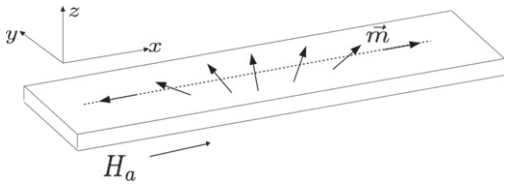

Fig. 2: Coordinate axes and applied field on a thin strip. Under the action of the applied field the unit magnetization vector $\vec{m}$ will rotate having a small z component if the hard-axis anisotropy is large.

asymptotic dynamics predicts a transition from a Walker-type regime to a regime where the speed increases with the square root of the applied field. In leading order the dynamics of the in-plane magnetization obeys a reaction diffusion equation, and the magnetization in the hard-axis direction is slaved to the in-plane components. The new asymptotic regime appears as a transition from a pushed to a pulled front at a critical value of the applied field.

The starting point of the calculation is the LLG equation for the magnetization. The material has magnetization $\vec{M} = M_s\vec{m}$ where M_s is the saturation magnetization and $\vec{m} = (m_1, m_2, m_3)$ is a unit vector along the direction of magnetization. The dynamic evolution of the magnetization is governed by the LLG equation,

$$\frac{\mathrm{d}\vec{M}}{\mathrm{d}t} = -\gamma_0\vec{M}\times\vec{H}_{\rm eff} + \alpha\frac{\vec{M}}{M_s}\times\frac{\mathrm{d}\vec{M}}{\mathrm{d}t}, \qquad (1)$$

where $\vec{H}_{\rm eff}$ is the effective magnetic field, $\gamma_0 = |\gamma|\mu_0$, γ is the gyromagnetic ratio of the electron and μ_0 is the magnetic permeability of vacuum. The constant $\alpha > 0$ is the dimensionless phenomenological Gilbert damping coefficient.

The problem that we will consider may describe either a biaxial nanowire with the easy axis along its length and a hard-axis along a transverse direction (which we choose as the z-axis as in fig. 1) or a thin and narrow film in the (x, y)-plane, with the easy axis x along its length and hard axis perpendicular to the thin-film plane. A constant external field is applied along the easy axis $\vec{H}_a = H_a\hat{x}$, as shown in figs. 1 and 2. For sufficiently hard-axis anisotropy the magnetization will lie predominantly in the (x, y)-plane having a small z component.

For a nanowire and for a thin narrow film the magnetization may be assumed [11] to depend on the easy-axis coordinate, $\vec{M}(x, y, z) = \vec{M}(x)$. The effective magnetic field is given by [5–9]

$$\vec{H}_{\rm eff} = H_a\hat{x} + \frac{C_{\rm ex}}{\mu_0 M_s^2}\frac{\partial^2\vec{M}}{\partial x^2} + \frac{2K_u}{\mu_0 M_s^2}M_1\hat{x} - \frac{2K_d}{\mu_0 M_s^2}M_3\hat{z}, \quad (2)$$

where $C_{\rm ex}$ is the exchange constant, K_u the easy-axis effective uniaxial anisotropy and K_d is an effective hard-axis anisotropy. We have assumed that the demagnetizing field has a local expression as an additional anisotropy in the direction perpendicular to the thin-film plane, as demonstrated rigorously in [12]. The combined effect of a local approximation for the demagnetizing field plus crystalline and stress-induced anisotropies may be represented by effective anisotropies [9].

Introducing M_s as unit of magnetic field, and introducing the dimensionless space and time variables $\xi = x\sqrt{K_u/C_{\rm ex}}$ and $\tau = \mu_0|\gamma|M_s t$ we rewrite eqs. (1) and (2) in dimensionless form

$$\frac{\mathrm{d}\vec{m}}{\mathrm{d}\tau} = -\vec{m}\times\vec{h}_{\rm eff} + \alpha\vec{m}\times\frac{\mathrm{d}\vec{m}}{\mathrm{d}\tau} \qquad (3)$$

with

$$\vec{h}_{\rm eff} = h_a\hat{x} + \frac{1}{2}K_\parallel\frac{\partial^2\vec{m}}{\partial\xi^2} + K_\parallel m_1\hat{x} - K_\perp m_3\hat{z}, \qquad (4)$$

where h_a is the dimensionless applied field and the dimensionless numbers that have appeared are $K_\parallel = 2K_u/(\mu_0 M_s^2)$, $K_\perp = 2K_d/(\mu_0 M_s^2)$. Equations (3) and (4) describe the dynamics of the problem.

We are interested in the case of a perpendicular (z-axis) anisotropy much larger than the uniaxial anisotropy. We will also assume that the dimensionless applied field is weak. We search then for a solution of the LLG equation in the asymptotic limit $h_a \ll K_\perp$, $K_\parallel \ll K_\perp$ and therefore, $m_1, m_2 \gg m_3$. Let then $m_1 = m_{10} + \epsilon m_{11} + \ldots$, $m_2 = m_{20} + \epsilon m_{21} + \ldots$, $m_3 = \epsilon m_{30} + \epsilon^2 m_{31} + \ldots$, where ϵ is a small quantity. Since the perpendicular anisotropy is larger than the uniaxial anisotropy and the applied field is weak, we introduce the scaling $K_\parallel = \epsilon\tilde{K}_\parallel$, $h_a = \epsilon\tilde{h}_a$ with $K_\perp$ of order one. The components of the effective magnetic field, $\vec{h}_{\rm eff} = (h_1, h_2, h_3)$ become then $h_i = \epsilon h_{i0} + \epsilon^2 h_{i1} + \ldots$ with the leading-order components given by

$$h_{10} = \tilde{h}_a + \frac{1}{2}\tilde{K}_\parallel\frac{\partial^2 m_{10}}{\partial\xi^2} + K_\parallel m_{10}, \qquad (5a)$$

$$h_{20} = \frac{1}{2}\tilde{K}_\parallel\frac{\partial^2 m_{20}}{\partial\xi^2} \quad \text{and} \qquad (5b)$$

$$h_{30} = -K_\perp m_{30}. \qquad (5c)$$

Furthermore we introduce a slow time scale $s = \epsilon\tau$ and notice that the leading-order components of the in-plane magnetization satisfy

$$m_{10}^2 + m_{20}^2 = 1 - O(\epsilon^2). \qquad (6)$$

Introducing these scalings in eq. (3) and expanding in ϵ one obtains in leading order,

$$\frac{\partial m_{10}}{\partial s} = -m_{20}h_{30}, \tag{7a}$$

$$\frac{\partial m_{20}}{\partial s} = m_{10}h_{30}, \tag{7b}$$

$$0 = -m_{10}h_{20} + m_{20}h_{10} + \alpha\left(m_{10}\frac{\partial m_{20}}{\partial s} - m_{20}\frac{\partial m_{10}}{\partial s}\right). \tag{7c}$$

Substituting (7a) and (7b) into (7c) and using (6) we find that in leading order,

$$h_{30} = \frac{1}{\alpha}(m_{10}h_{20} - m_{20}h_{10}) \tag{8}$$

and eqs. (7a) and (7b) become

$$\frac{\partial m_{10}}{\partial s} = -\frac{m_{20}}{\alpha}(m_{10}h_{20} - m_{20}h_{10}), \tag{9a}$$

$$\frac{\partial m_{20}}{\partial s} = \frac{m_{10}}{\alpha}(m_{10}h_{20} - m_{20}h_{10}). \tag{9b}$$

Because of (6) we can write $m_{10} = \cos\theta$, $m_{20} = \sin\theta$. Using (5a) in eqs. (8), (9) we obtain

$$\alpha\frac{\partial\theta}{\partial s} = \frac{1}{2}\tilde{K}_\parallel\theta_{\xi\xi} - \sin\theta(\tilde{h}_a + \tilde{K}_\parallel\cos\theta), \tag{10}$$

$$m_{30} = -\frac{1}{K_\perp}\frac{\partial\theta}{\partial s}. \tag{11}$$

Finally going back to the unscaled time variable τ and parameters $K_\parallel, K_\perp$, we write the leading-order magnetization components as

$$m_1 = \cos\theta, \quad m_2 = \sin\theta, \quad m_3 = -\frac{1}{K_\perp}\frac{\partial\theta}{\partial\tau}, \tag{12a}$$

where

$$\alpha\frac{\partial\theta}{\partial\tau} = \frac{K_\parallel}{2}\theta_{\xi\xi} - \sin\theta(h_a + K_\parallel\cos\theta). \tag{12b}$$

Equations (12) show that the leading-order dynamics is determined by the equation for the in-plane magnetization components, the perpendicular magnetization is slaved to the tangential magnetization. Equation (12b) is the well-studied reaction diffusion equation, for which we know that an initial perturbation to an unstable state evolves into the monotonic front of minimal speed [13]. In order to render (12b) into the standard form we introduce the dependent variable u defined by $\theta = \pi(1-u)$ which satisfies

$$\alpha u_\tau = Du_{\xi\xi} + f(u), \tag{13}$$

with

$$f(u) = \frac{1}{\pi}\sin\pi u(h_a - K_\parallel\cos\pi u).$$

The diffusion constant $D = K_\parallel/2$ and the reaction term f satisifies $f(u) > 0$ in (0,1), $f(0) = f(1) = 0$. A small perturbation to the unstable state $u = 0$ ($\theta = \pi$) evolves into a traveling monotonic front of minimal speed c^* [13,14] that joins the unstable state to the stable state $u = 1(\theta = 0)$. The minimal speed can be obtained from a variational principle [15] and is bounded by [13]

$$c_{\mathrm{KPP}} \equiv \frac{2}{\alpha}\sqrt{Df'(0)} < c^* < \frac{2}{\alpha}\sqrt{D\sup f(u)/u}. \tag{14}$$

When the upper and lower bounds coincide the speed is exactly c_{KPP} and the traveling front is called a KPP or pulled front. The dynamics associated to this equation has been studied for its mathematical interest and for its application in population dynamics, autocatalytic chemical reactions and others. We refer to [16] for a description of some of its mathematical features and biological applications and to [17] for a recent review.

In the present problem eq. (13) has the exact traveling front solution

$$u(\xi,\tau) = \frac{2}{\pi}\arctan\left[\mathrm{e}^{-\sqrt{\frac{K_\parallel}{D}}(\xi - c_{\mathrm{N}}\tau)}\right], \tag{15}$$

where

$$c_{\mathrm{N}} = \frac{h_a}{\alpha}\sqrt{\frac{D}{K_\parallel}}.$$

This solution is not a KPP front, it is a so-called pushed front, that is, it does not propagate with the KPP speed. This is the front into which an initial condition will evolve only if it is the front of minimal speed. It is not difficult to verify that as h_a increases this is not the the front of minimal speed and an initial condition $u(x,0)$ will not evolve into this solution. For $h_a \geq 4K_\parallel$ the upper and lower bounds in (14) coincide and the speed of the front must be the KPP value. The transition from a pushed to a pulled front may occur before the upper and lower bounds coincide. In this problem for which there is an exact solution we know that the transition will occur when $c_{\mathrm{N}} = c_{\mathrm{KPP}}$. That is

$$c = \begin{cases} \dfrac{h_a}{\alpha}\sqrt{\dfrac{D}{K_\parallel}}, & \text{if } h_a \leq 2K_\parallel, \\ \dfrac{2}{\alpha}\sqrt{D(h_a - K_\parallel)}, & \text{if } h_a > 2K_\parallel. \end{cases}$$

Going back to the physical variables, we have then that the speed of the domain wall is given by

$$v = \begin{cases} \dfrac{1}{\alpha}\sqrt{\dfrac{C_{\mathrm{ex}}}{2K_u}}\mu_0|\gamma|H_a, & \text{if } H_a < \dfrac{4K_u}{\mu_0 M_s}, \\ \dfrac{2|\gamma|\sqrt{C_{\mathrm{ex}}}}{\alpha M_s}\sqrt{\mu_0 M_s H_a - 2K_u}, & \text{if } H_a > \dfrac{4K_u}{\mu_0 M_s}. \end{cases} \tag{16}$$

In the small-field regime $H_a < H_c = 4K_u/(\mu_0 M_s)$ the magnetization profile is obtained from (15) and it is

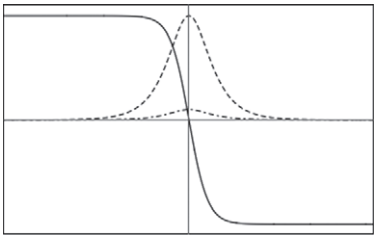

Fig. 3: Graph of the magnetization profile eq. (17). The solid line corresponds to m_1, the dashed line to m_2 and the dotted line shows the small m_3 component.

given by

$$m_1 = \tanh\left[-\frac{(x-vt)}{\Delta}\right], \tag{17a}$$

$$m_2 = \operatorname{sech}\left[\frac{(x-vt)}{\Delta}\right], \tag{17b}$$

$$m_3 = \frac{\mu_0 M_s H_a}{\sqrt{2}\alpha K_d}\operatorname{sech}\left[\frac{(x-vt)}{\Delta}\right], \tag{17c}$$

where the domain wall width is given by $\Delta = (1/2)\sqrt{C_{\rm ex}/K_u}$. In fig. 3 we show the components of the traveling domain wall.

For an applied field larger than H_c there is no analytical expression for the front profile, only the speed has an explicit analytic formula. The general theory of reaction diffusion equations [13,14] guarantees its existence, that it is a monotonic decaying front and that it approaches the fixed points exponentially. It is similar in shape to (15) but it does not have an explicit analytic expression in this problem.

The solution that we find, eq. (15), corresponds to the limit of the Schryer-Walker solution when the magnetization lies predominantly in the plane defined by the easy axis and the applied magnetic field. The Schryer-Walker solution is given by

$$\begin{aligned}\sin 2\varphi_0 &= H_0/(2\pi\alpha M_0) = H_0/H_W,\\ \log\tan\frac{1}{2}\theta &= [1+(2\pi M_0^2/K)\cos^2\varphi_0]^{1/2}(x-vt),\\ v &= (-\gamma H_0/\alpha)[1+(2\pi M_0^2/K)\cos^2\varphi_0]^{-1/2},\end{aligned}$$

where $\gamma < 0$, the demagnetizing field is $4\pi M_x$ and $H_W = 2\pi\alpha M_0$ is the Walker critical field. For $h = H_0/M_0 \approx \mathcal{O}(\epsilon)$ we have $\varphi_0 = \pi/2 - \epsilon$. One can verify that $1+(2\pi M_0^2/K)\cos^2\varphi_0 = 1+\mathcal{O}(\epsilon)\approx 1$ where we have also used the fact that K/M_0^2 is of order ϵ. In this limit the Schryer-Walker solution coincides with (15).

Equations (16) and (17) constitute our main result.

These results, obtained from the LLG equation in the case $K_\parallel \ll K_\perp$ and for a weak applied field, explain qualitatively the results of the numerical simulations [5–7], of the experiments [9] and the stability results [8]. At low fields the speed of the front is proportional to the applied field H_a and inversely proportional to the damping coefficient α. The magnetization profile and the speed share the main features of the Walker solution, the velocity shows linear dependence on the applied field and inverse proportionality on the damping constant α. The Walker breakdown field $H_W = \alpha K_\perp/2$ is of order one, and therefore large compared to the transition field H_c. Thus, we recover the behavior described in [5–8]: for sufficiently large perpendicular anisotropy the Walker solution loses stability before the breakdown field to a domain wall of slower increasing speed with the field. When the applied field is weak and $K_\parallel \ll K_\perp$ the numerical integrations in [5,7] show that the speed increases slowly with the field once the Walker solution loses stability, in agreement with the results found in this work. The experimental results for sample A3 at a temperature $T = 20\,\mathrm{K}$ obtained in [9] are consistent with the results obtained in the present work.

The asymptotic approach that we have used is based on [10], where the numerical simulations, (although for a different demagnetizing field), show that the asymptotic dynamics reproduces the relaxation dynamics of the full LLG equation, filtering out the spin waves. Reaction diffusion dynamics has also been encountered in thin nanotubes [18], where the Walker breakdown is not observed. A transition from a linearly increasing to a slower increasing domain wall speed also occurs in thin nanotubes as reported in [19,20]. The asymptotic dynamics of the LLG equation has been studied by several authors in different limiting parameter ranges, and wave-type motion governed by other evolution equations has been derived [21,22]. In particular, different approximations to the demagnetizing field of a thin film have been studied. Here we use the local approximation derived in [12], we refer to [23] for a review of the different scaling regimes and the corresponding effective fields. In the present problem we have chosen a parameter regime for which recent numerical and experimental work has been performed and found qualitative agreement with the results reported in them.

* * *

This work has been partially supported by Fondecyt (Chile) projects 1141155 and Iniciativa Científica Milenio, ICM (Chile), through the Millenium Nucleus RC120002.

REFERENCES

[1] Stamps R. L. *et al.*, *J. Phys. D: Appl. Phys.*, **47** (2014) 333001.
[2] Landau L. D. and Lifshitz E. M., *Phys. Z. Sowjet.*, **8** (1935) 153.
[3] Gilbert T. L., *IEEE Trans. Magn.*, **40** (2004) 3443.
[4] Schryer N. L. and Walker L. R., *J. Appl. Phys.*, **45** (1974) 5406.
[5] Wieser R., Vedmedenko E. Y. and Wiesendanger R., *Phys. Rev. B*, **81** (2010) 024405.
[6] Wang X. S., Yan P., Shen Y. H., Bauer G. E. and Wang X. R., *Phys. Rev. Lett.*, **109** (2012) 167209.

[7] Wang X. S. and Wang X. R., *Phys. Rev. B*, **90** (2014) 184415.
[8] Hu B. and Wang X. R., *Phys. Rev. Lett.*, **111** (2013) 027205.
[9] Thevenard L., Hussain S. A., von Bardeleben H. J., Bernard M., Lemaître A. and Gourdon C., *Phys. Rev. B*, **85** (2012) 064419.
[10] García Cervera C. J. and E W. N., *J. Appl. Phys.*, **90** (2001) 370.
[11] Porter D. G. and Donahue M. J., *J. Appl. Phys.*, **95** (2004) 6729.
[12] Gioia G. and James R. D., *Proc. R. Soc. Lond. A*, **453** (1997) 213.
[13] Aronson D. G. and Weinberger H. F., *Adv. Math.*, **30** (1978) 33.
[14] Kolmogorov A. N., Petrovskii I. G. and Piskunov N. S., *Selected Works of A. N. Kolmogorov*, edited by Tikhomirov V. M. (Kluwer Academic Publishers) 1991.
[15] Benguria R. D. and Depassier M. C., *Phys. Rev. Lett.*, **77** (1996) 1171.
[16] Murray J. D., *Mathematical Biology* (Springer, Berlin) 1989.
[17] Van Saarloos W., *Phys. Rep.*, **386** (2003) 29.
[18] Goussev A., Robbins J. M. and Slastikov V., *EPL*, **105** (2014) 67006.
[19] Yan M., Andreas C., Kákay A., García-Sánchez F. and Hertel R., *Appl. Phys. Lett.*, **99** (2011) 122505.
[20] Depassier M. C., *EPL*, **108** (2014) 37008.
[21] Mikeska H. J., *J. Appl. Phys.*, **52** (1981) 1950.
[22] Capella A., Melcher C. and Otto F., *Nonlinearity*, **20** (2007) 2519.
[23] DeSimone A., Kohn R. V., Muller S. and Otto F., in *The Science of Hysteresis: Physical modeling, Micromagnetics, and Magnetization Dynamics*, edited by Bertotti G. and Mayergoyz I. D., Vol. **2** (Gulf Professional Publishing) 2006.